The Long Non-coding RNA *Cyrano* Is Dispensable for Pluripotency of Murine and Human Pluripotent Stem Cells

Hannah J. Hunkler,[1] Jeannine Hoepfner,[1] Cheng-Kai Huang,[1] Shambhabi Chatterjee,[1] Monica Jara-Avaca,[2,3] Ina Gruh,[2,3] Emiliano Bolesani,[2,3] Robert Zweigerdt,[2,3] Thomas Thum,[1,2,4] and Christian Bär[1,2,*]

[1]Institute of Molecular and Translational Therapeutic Strategies (IMTTS), Hannover Medical School, Hannover, Germany
[2]REBIRTH-Centre for Translational Regenerative Medicine, Hannover Medical School, Hannover, Germany
[3]Leibniz Research Laboratories for Biotechnology and Artificial Organs (LEBAO), Department of Cardiac, Thoracic-, Transplantation and Vascular Surgery, Hannover Medical School, Hannover, Germany
[4]Co-senior author
*Correspondence: baer.christian@mh-hannover.de
https://doi.org/10.1016/j.stemcr.2020.05.011

SUMMARY

Pluripotency is tightly regulated and is crucial for stem cells and their implementation for regenerative medicine. Non-coding RNAs, especially long non-coding RNAs (lncRNAs) emerged as orchestrators of versatile (patho)-physiological processes on the transcriptional and post-transcriptional level. *Cyrano*, a well-conserved lncRNA, is highly expressed in stem cells suggesting an important role in pluripotency, which we aimed to investigate in loss-off-function (LOF) experiments. *Cyrano* was described previously to be essential for the maintenance of mouse embryonic stem cell (ESC) pluripotency. In contrast, using different genetic models, we here found *Cyrano* to be dispensable in murine and human iPSCs and in human ESCs. RNA sequencing revealed only a moderate influence of *Cyrano* on the global transcriptome. In line, *Cyrano*-depleted iPSCs retained the potential to differentiate into the three germ layers. In conclusion, different methods were applied for LOF studies to rule out potential off-target effects. These approaches revealed that *Cyrano* does not impact pluripotency.

INTRODUCTION

The use of embryonic stem cells (ESCs) has been an invaluable tool for basic cell and biomedical research for more than two decades. The discovery of cellular reprogramming of somatic cells into induced pluripotent stem cells (iPSCs) (Takahashi and Yamanaka, 2006) revolutionized the field of regenerative medicine. These iPSCs can be generated from patient material and subsequently differentiated into a desired cell type for allogenic or ideally autologous cell therapy. In addition, iPSC technology enabled disease-in-a-dish modeling, for example, to better understand monogenetic disorders or to perform drug screenings in a personalized manner.

In stem cells the maintenance of pluripotency and self-renewal are crucial processes necessary to retain the differentiation capacity into various cell types of the three germ layers. In addition to the core pluripotency factors Oct4, Sox2, and Nanog, chromatin- and RNA-mediated mechanisms are involved in the regulation of pluripotency, which are not yet fully understood (Li and Belmonte, 2017). During differentiation, pluripotency and developmental genes undergo various changes, including altered chromatin interactions, histone modifications, and subnuclear localization. This leads to a change in expression patterns of genes connected to pluripotency, features of stem cells, and differentiated cell types.

Another level of complexity in the regulation of pluripotency is added by non-coding RNAs (ncRNAs), including microRNAs (miRNAs), long non-coding RNAs (lncRNAs), and circular RNA. lncRNAs constitute the largest and most heterogeneous subclass of ncRNAs classified by a transcript length of over 200 nucleotides. They play crucial roles in many physiological and pathophysiological processes (Beermann et al., 2016) and regulate gene expression transcriptionally and post-transcriptionally by manifold mechanisms (Bär et al., 2016; Nelson et al., 2016). However, due to their large number (lncipedia.org currently annotates 56,946 human lncRNA genes) and diversity, lncRNA research is still in its infancy and many lncRNA-controlled processes remain elusive. Additional challenges for studying lncRNAs are their frequently low level of expression and relatively poor sequence conservation, even between closely related species.

In contrast, lncRNA *Cyrano* (*OIP5-AS1*) is both locus- and sequence-conserved with a high complementary miRNA-7 binding site in an ultra-conserved region (Ulitsky et al., 2011). *Cyrano* was first described in zebrafish embryogenesis, necessary for the development of eyes and brain (Ulitsky et al., 2011). In HeLa cells *Cyrano* acts as a sponge for the RNA-binding protein HuR which influences proliferation. If HuR is not sponged by *Cyrano*, it stabilizes its target mRNAs, which code for pro-proliferative proteins, such as cyclin A2 and D1 (Kim et al., 2016). Apoptosis is regulated by *Cyrano* in vascular endothelial cells upon treatment with oxidative low-density lipoprotein (Wang et al., 2019). Moreover, *Cyrano* is part of a regulatory network of ncRNAs, including miRNA-7 in murine brains (Kleaveland
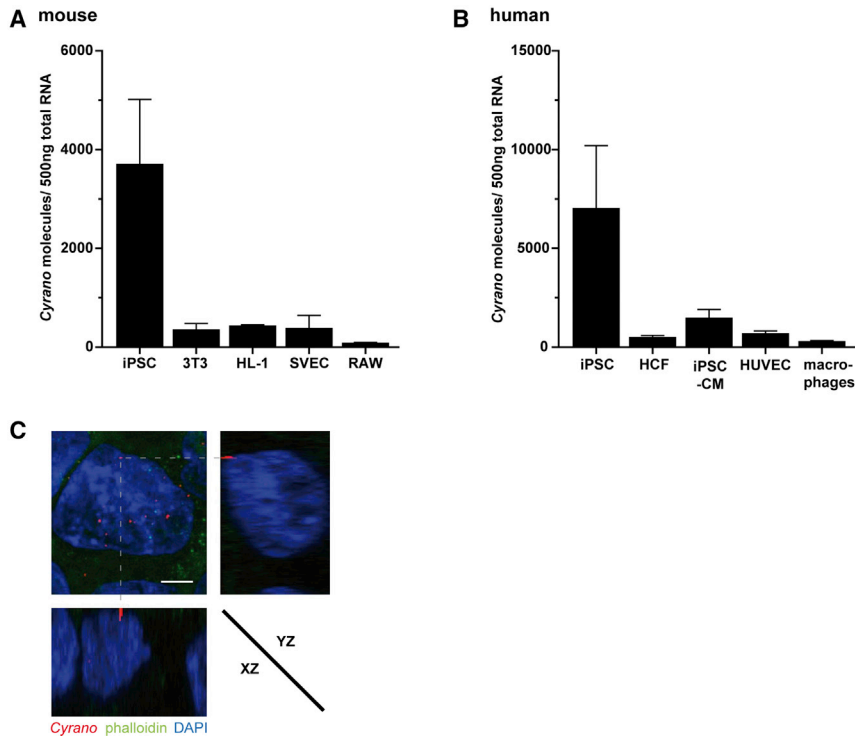
Figure 1. *Cyrano* Is Highly Enriched in iPSCs

Absolute quantification of murine (A) and human (B) *Cyrano* in different cell lines. qRT-PCR and a plasmid standard containing parts of murine or human *Cyrano* were used for quantification, n = 3 technical replicates. SVEC, seminal vesicle epithelial cells; RAW264.7 macrophages; HCF, human cardiac fibroblasts; iPSC-CM, iPSC-derived cardiomyocytes; HUVEC, human umbilical vein endothelial cells; macrophages, peripheral blood mononuclear cell-derived macrophages.

(C) Representative RNA FISH images stained with a *Cyrano*-specific probe and phalloidin in unmodified human iPSCs as 3D reconstruction. Scale bar, 5 μm.

et al., 2018), and a regulatory role in pluripotency and self-renewal via miRNA-7 was proposed in murine ESCs (Smith et al., 2017).

The high conservation of *Cyrano* between vertebrates and its stem cell-enriched expression suggested an important regulatory role of this lncRNA, which prompted us to generate *Cyrano* knockout (KO) iPSCs. Surprisingly, *Cyrano* was concurrently described as an essential lncRNA for the maintenance of pluripotency and self-renewal in ESCs (Smith et al., 2017). Since this was in marked contrast to our results in *Cyrano* KO iPSCs, we decided to further investigate the specific role of *Cyrano* in pluripotency and self-renewal using different CRISPR/Cas9 and small interfering RNA (siRNA) approaches in murine and human PSCs.

RESULTS

Cyrano Is Highly Expressed in iPSCs

The remarkable species conservation prompted us to quantify *Cyrano* molecules in commonly used murine and human cell lines, as the expression of lncRNAs is often cell-type-specific (Beermann et al., 2016). A plasmid standard containing a sequence of the murine or human *Cyrano* transcript, respectively, was used for absolute quantification by qRT-PCR. Both human and murine *Cyrano* were strongly enriched in iPSCs compared with somatic cell lines (Figures 1A and 1B). RNA fluorescence in situ hybrid-

ization (FISH) with a *Cyrano*-specific probe followed by confocal microscopy and 3D reconstruction revealed a cytoplasmic localization in iPSCs (Figures 1C and S1).

Cyrano Is Dispensable for Maintenance of Pluripotency in Murine iPSCs

To address the role of *Cyrano* in pluripotency, OG2 iPSCs (expressing a pOCT4-EGFP transgene) (Kensah et al., 2013) were used to generate *Cyrano* KO cells by a dual guide RNA (gRNA) CRISPR/Cas9 approach (Heckl et al., 2014) (Figure 2A). The gRNAs were designed to excise the first exon of *Cyrano*, including parts of the promoter (Figure 2B). The dual gRNA vector, which also carries a dTomato fluorescence marker, was transiently transfected into OG2 iPSCs. Transfected cells were sorted by FACS and seeded as single cells for clonal expansion. Homo- and heterozygous KO clones for both gRNA combinations were identified by PCR in genomic DNA (Figure 2C) and successful excision confirmed by Sanger sequencing (Figure 2D). One heterozygous and one homozygous KO clone were selected for further analysis which, as expected, showed a significant reduction or complete elimination of *Cyrano* RNA expression as determined by qRT-PCR (Figure 2E).

Based on a previous report linking *Cyrano* to pluripotency maintenance (Smith et al., 2017), *Cyrano* KO iPSCs were analyzed for their pluripotency. The morphology of the cells appeared regular for iPSCs and the expression of
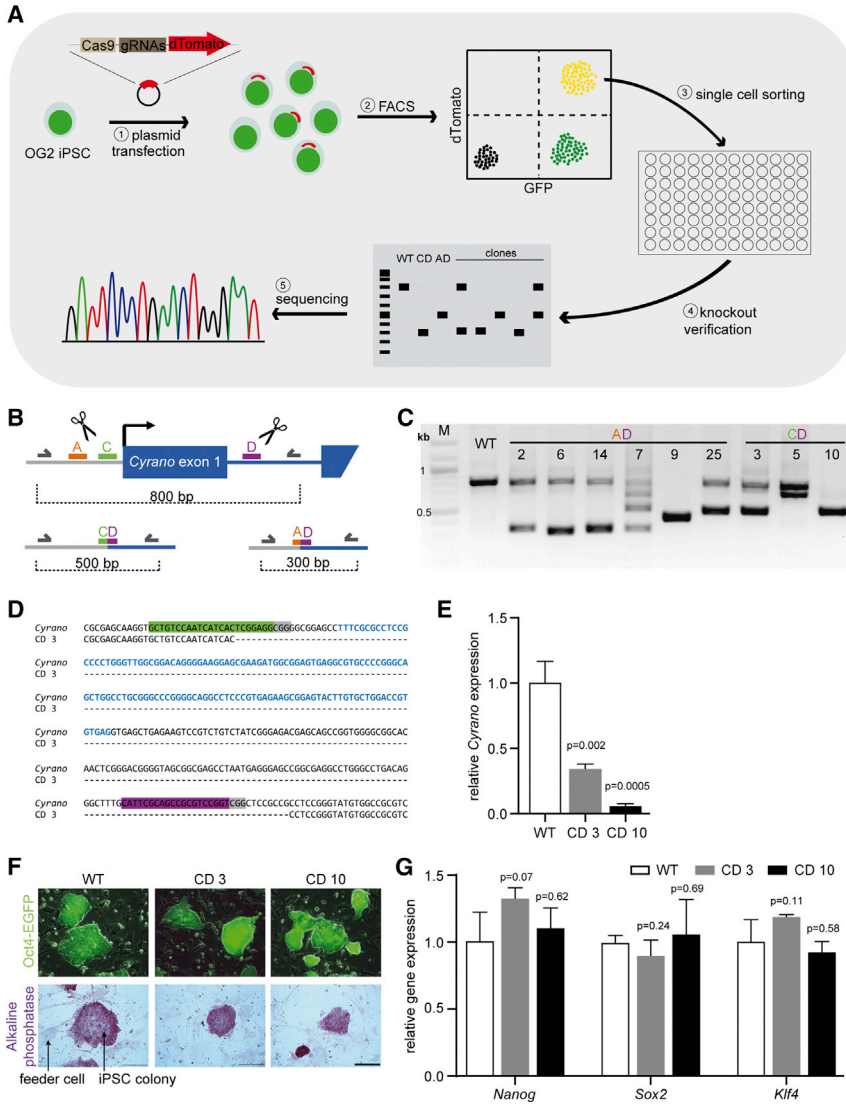
Figure 2. *Cyrano* Is Dispensable for Self-Renewal and Maintenance of Pluripotency in *Cyrano* KO Murine iPSCs

(A) Schematic overview of the generation of murine *Cyrano* KO iPSCs by CRISPR/Cas9.

(B) Graphical representation of three gRNAs (A, C, D) up- and downstream of the first exon of *Cyrano*. Primers used for PCR and sequencing are depicted as gray arrows, which amplify fragments of 800 bp in wild-type (WT) and 500 bp (using gRNA C and D) or 300 bp (using gRNA A and D) after CRISPR/Cas9 excision.

(C) Verification of *Cyrano* KO via PCR. Unmodified cells were loaded as control (WT).

(D) Example of Sanger sequencing results of clone CD 3 compared with WT *Cyrano* sequence. gRNA sequences are highlighted in green and purple with PAM sequences in gray, the sequence of the first exon is depicted in blue letters.

(E and G) Relative expression levels in KO and unmodified cells (WT). Expression levels were measured by qPCR, mean ± SD of three independent experiments are shown, unpaired t test was performed for statistical analysis.

(F) Representative images Oct4-EGFP expression and alkaline phosphatase staining of KO and unmodified cells (WT). iPSCs were cultured on feeder cells. Scale bar, 100 μm.

pOCT4-EGFP showed no differences. In addition, the expression of alkaline phosphatase was not altered in *Cyrano* KO iPSCs compared with wild-type iPSCs (Figure 2F). The mRNA expression levels of *Nanog*, *Sox2*, and *Klf4* did not change in response to the loss of *Cyrano* (Figure 2G). Thus, our data demonstrate that *Cyrano* is not required for pluripotency in murine iPSCs.

Knockdown of *Cyrano* Does Not Interfere with Pluripotency in Human iPSCs

We next set out to investigate the role of *Cyrano* in human iPSCs. In contrast to the genetic KO approach in murine iPSCs, a CRISPRi system (Mandegar et al., 2016) was used for inducible, highly efficient *Cyrano* knockdown (KD) (Figure 3A). Five different gRNAs, located around 150 bp up- and downstream of the transcription start site were designed, cloned into pgRNA-CKB, and nucleofected into CRISPRi iPSCs (Figure S2A). Bulk RNA expression analysis after dCas9 induction by doxycycline showed a significant downregulation of *Cyrano* for gRNA3 (Figure S2B). After clonal expansion, 21 colonies were treated with doxycycline to shut down *Cyrano* expression, which did not result in morphological abnormalities. Four clones were selected for further analyses based on their strong repression of *Cyrano* (Figure S2C). The nearly complete ablation of *Cyrano* was verified by RNA FISH. Specific *Cyrano* signals were comparable in control cells (no doxycycline or no gRNA), whereas hardly any signal was detected in *Cyrano* KD cells after doxycycline treatment (Figure 3B).

To exclude doxycycline-specific effects, CRISPRi iPSCs without a gRNA were treated with doxycycline. No effects
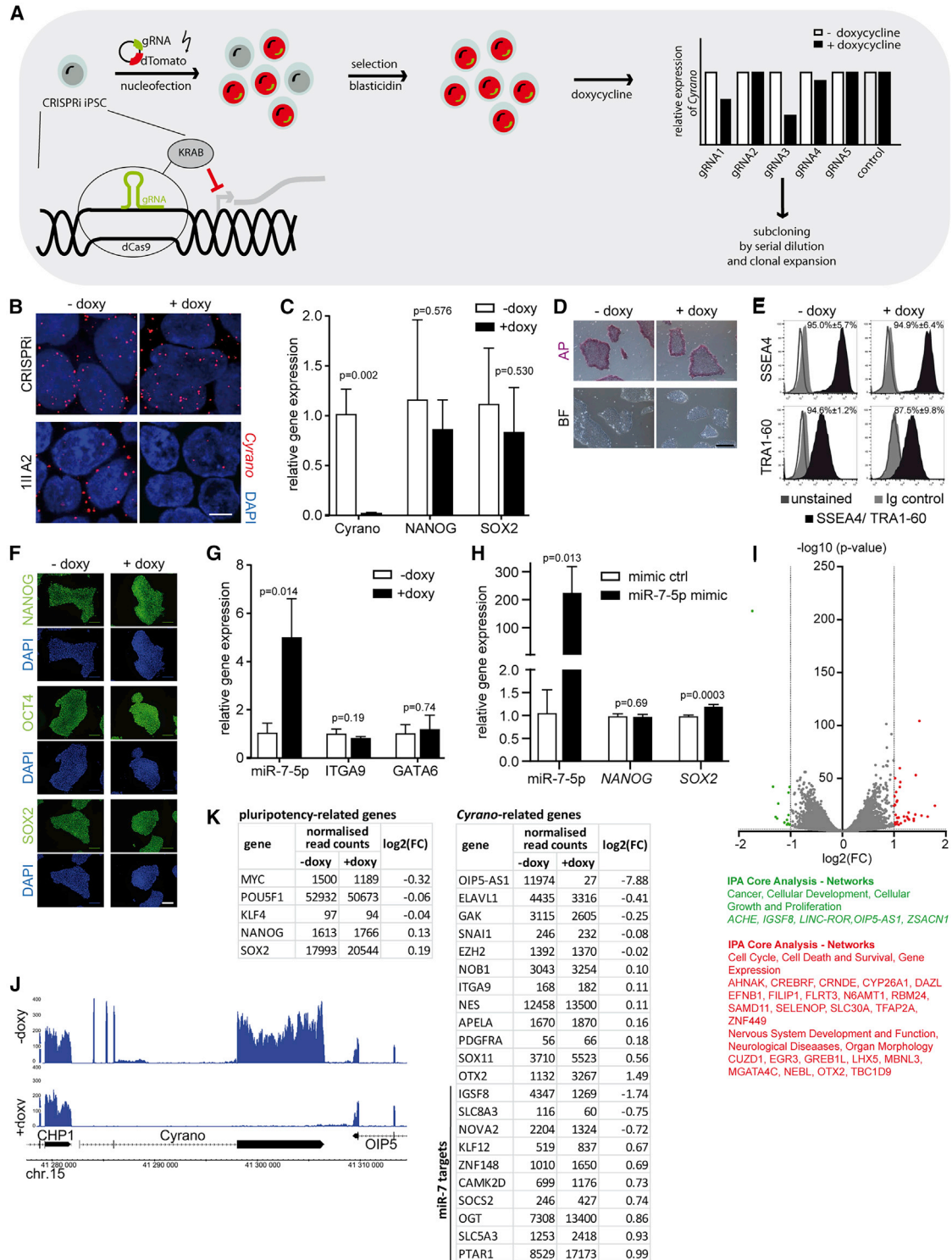
K

pluripotency-related genes

gene	normalised read counts		log2(FC)
	-doxy	+doxy	
MYC	1500	1189	-0.32
POU5F1	52932	50673	-0.06
KLF4	97	94	-0.04
NANOG	1613	1766	0.13
SOX2	17993	20544	0.19

Cyrano-related genes

gene	normalised read counts		log2(FC)
	-doxy	+doxy	
OIP5-AS1	11974	27	-7.88
ELAVL1	4435	3316	-0.41
GAK	3115	2605	-0.25
SNAI1	246	232	-0.08
EZH2	1392	1370	-0.02
NOB1	3043	3254	0.10
ITGA9	168	182	0.11
NES	12458	13500	0.11
APELA	1670	1870	0.16
PDGFRA	56	66	0.18
SOX11	3710	5523	0.56
OTX2	1132	3267	1.49
IGSF8	4347	1269	-1.74
SLC8A3	116	60	-0.75
NOVA2	2204	1324	-0.72
KLF12	519	837	0.67
ZNF148	1010	1650	0.69
CAMK2D	699	1176	0.73
SOCS2	246	427	0.74
OGT	7308	13400	0.86
SLC5A3	1253	2418	0.93
PTAR1	8529	17173	0.99

miR-7 targets

IPA Core Analysis - Networks
Cancer, Cellular Development, Cellular
Growth and Proliferation
ACHE, IGSF8, LINC-ROR, OIP5-AS1, ZSACN1

IPA Core Analysis - Networks
Cell Cycle, Cell Death and Survival, Gene
Expression
AHNAK, CREBRF, CRNDE, CYP26A1, DAZL
EFNB1, FILIP1, FLRT3, N6AMT1, RBM24,
SAMD11, SELENOP, SLC30A, TFAP2A,
ZNF449
Nervous System Development and Function,
Neurological Diseaases, Organ Morphology
CUZD1, EGR3, GREB1L, LHX5, MBNL3,
MGATA4C, NEBL, OTX2, TBC1D9

Figure 3. KD of *Cyrano* with CRISPRi Approach Has No Impact on the Pluripotency of Human iPSCs
(A) Schematic overview of the generation of inducible *Cyrano* KD human iPSCs using a CRISPRi approach.
(B) Representative RNA FISH images stained with a *Cyrano*-specific probe in unmodified cells (CRISPRi) and one clone, with and without doxycycline (doxy) treatment. Nuclei were stained with DAPI. Scale bar, 5 μm.

(legend continued on next page)

were observed with regard to growth dynamics, expression of pluripotency markers, or alkaline phosphatase staining (Figures S2D–S2G).

Similar to the observation in murine iPSCs, the expression levels of *NANOG* and *SOX2* were unchanged after doxycycline-induced *Cyrano* KD (Figures 3C and S3A). Furthermore, neither the alkaline phosphatase staining, nor the morphology of the cells showed any changes after *Cyrano* KD (Figures 3D and S3B). The proliferation dynamics were also unaffected by the loss of *Cyrano* (Figure S3C). The pluripotency markers SSEA4 and TRA1-60 were analyzed by flow cytometry, and NANOG, OCT4, and SOX2 by immunohistochemistry. These markers did not respond to loss of *Cyrano* (Figures 3E, 3F, S3D, and S3E). Since *Cyrano* was shown to act on miR-7-5p in murine ESCs, which in turn represses *Nanog* and *Itga9*, it was therefore suggested to influence pluripotency and cell adhesion (Smith et al., 2017). We checked the expression of miR-7-5p, its proposed target *ITGA9*, and *GATA6* as a negatively regulated target of *NANOG*, and saw that silencing *Cyrano* significantly increased only miR-7-5p levels, while *ITGA9* and *GATA6* remained unaffected (Figures 3G and S3F). In addition, iPSC treatment with miR-7-5p mimics had no consequences on *NANOG* (a suggested direct target of miR-7) or on *SOX2* expression (Figure 3H). Consequently, alkaline phosphatase staining after miR-7 overexpression was indifferent from mimic controls (Figure S3G).

Loss of *Cyrano* Only Moderately Affects the Global Transcriptome

Transcriptome analysis in human iPSCs with and without doxycycline treatment, i.e., in the presence and absence of *Cyrano,* led to differential expression of only 50 genes: 34 genes were up- and 16 downregulated ($-1 < \log2(FC) > 1$, $p < 0.01$) (Figures 3I and S4A). Using Ingenuity Pathway Analysis (IPA), downregulated genes are linked to the "cancer, cellular development, cellular growth and proliferation"

network while upregulated genes are part of the "cell cycle, cell death and survival, gene expression," or "nervous system development and function, neurological disease, organ morphology" networks (Figure 3I). As shown in the RNA sequencing (RNA-seq) read mapping in a genome browser, *Cyrano* is nearly absent after doxycycline treatment. This had no effect on the neighboring genes *CHP1* and *OIP5*, indicating that off-target effects in *cis* can be ruled out (Figures 3J and S4B). Figure 3K shows normalized RNA-seq read-count tables for genes related to pluripotency or connected to *Cyrano* based on literature research (more genes in Figure S4C). None of them were significantly dysregulated after *Cyrano* KD except for orthodenticle homeobox 2 (*OTX2*), which is a transcription factor in brain development (Beby and Lamonerie, 2013). In line with higher levels of miR-7 after *Cyrano* KD (Figure 3G), some known miR-7 targets (IGFS8, SLC8A3) (Agarwal et al., 2015) were downregulated, but none have been linked to pluripotency. The RNA-seq data were validated by qRT-PCR measurements (Figure S4D). Finally, to further demonstrate that *Cyrano* is dispensable for pluripotency, we performed a trilineage differentiation assay. Importantly, loss of *Cyrano* did not influence the potential of human iPSC to differentiate into the three different germ layers (Figures 4A and S4E).

Inhibition of *Cyrano* in Human ESCs by siRNA Has No Effect on Pluripotency

Despite large similarities of ESCs and iPSCs in expression patterns and chromatin modifications, there are also certain differences in gene expression and methylation profiles (Bilic and Belmonte, 2012). To test whether *Cyrano* is specifically required for the maintenance of pluripotency in human ESCs, we used an siRNA approach to silence *Cyrano* in these cells. *NANOG* and *SOX2* remained unchanged after silencing (Figure 4B) and the expression of SSEA4 and TRA1-60 did not change after *Cyrano* modulation (Figure 4C).

(C) Expression of *Cyrano*, *NANOG*, and *SOX2* after doxy treatment in the monoclonal population. Expression levels were measured by qRT-PCR, mean ± SD of three independent experiments are shown, unpaired t test was performed for statistical analysis.

(D) Representative images of alkaline phosphatase staining of one KD clone with and without doxy treatment. Scale bar, 500 μm.

(E) Flow cytometry analysis of SSEA4 and TRA1-60 of one clone. Isotype controls (light gray, filled) and unstained cells (dark gray line) were used as controls. Representative plots with mean ± SD of three independent experiments are depicted.

(F) Fluorescence immunocytochemistry of NANOG, OCT4, and SOX2 was performed in *Cyrano* KD cells after doxy treatment. Scale bar, 100 μm.

(G) Expression levels were measured by qRT-PCR, mean ± SD of three independent experiments, unpaired t test was performed for statistical analysis.

(H) miR-7-5p was overexpressed in CRISPRi cells. Expression levels were measured by qRT-PCR, mean ± SD of three independent experiments, unpaired t test was performed for statistical analysis.

(I) Volcano plot depicting the results of the RNA sequencing of *Cyrano* KD clone with and without doxy treatment of three experiments. Cut off criteria $-1 < \log2(FC) > 1$, q > 2. IPA network analysis.

(J) RNA-seq tracks of CRISPRi 1II E12 with and without doxy.

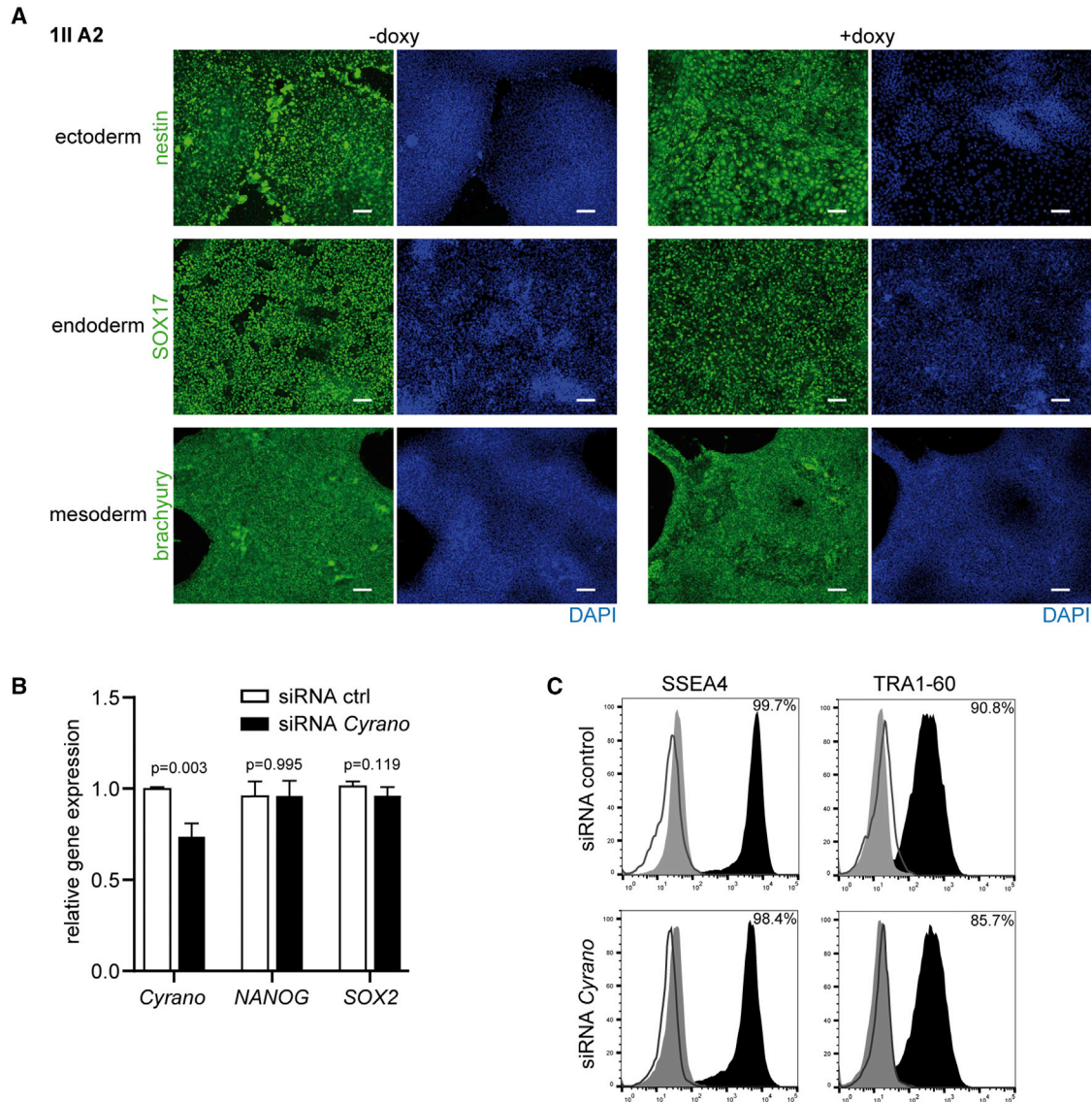(K) Normalized read counts using DEseq2 of pluripotency-related and *Cyrano*-related genes.

Figure 4. Silencing of *Cyrano* Does Not Influence the Differentiation Potential of Human iPSCs or Pluripotency of Human ESCs

(A) Differentiation of iPSCs in the presence and absence of *Cyrano* to the three germ layers with subsequent immunofluorescence staining. Scale bar, 100 μm.

(B) Gene expression of *Cyrano*, *NANOG*, and *SOX2* was analyzed by qRT-PCR, mean ± SD of three independent experiments, unpaired t test was performed for statistical analysis.

(C) Flow cytometry analysis of SSEA4 and TRA1-60 after *Cyrano* silencing in human ESCs. Isotype controls (filled gray) and unstained cells (dark gray line) were used as controls.

DISCUSSION

Here, we report that the highly conserved lncRNA *Cyrano* is enriched in PSCs which prompted us to investigate its functional role pluripotency. We used a dual gRNA CRISPR/Cas9 approach to generate a *Cyrano* KO in murine iPSCs, which did not result in adverse effects on pluripotency. This was in marked contrast to a simultaneously published report suggesting that *Cyrano* is essential for plu-

ripotency in murine ESCs (Smith et al., 2017). To have a more clinically translatable platform and to also strengthen our own data with a different approach, we used CRISPRi in human iPSCs for a robust KD of *Cyrano*. As a third model, we used human ESCs in which *Cyrano* was silenced with specific siRNAs. Both approaches confirmed the data from murine iPSCs, showing that *Cyrano* has no overt effect on pluripotency in stem cells from different species. As mentioned above, this is in contrast to previously

published data suggesting that *Cyrano* derepresses *Nanog* by sponging miR-7-5p. The two main differences between the studies were: firstly, Smith et al. investigated murine ESCs grown in potentially less-stringent stem cell culture conditions that may favor differentiation upon *Cyrano* repression. Nevertheless, when seeding human ESCs at low density, which can be considered a less-stringent condition, no effect after siRNA *Cyrano* treatment was observed. Secondly, Smith et al. (2017) used commercially available small hairpin RNAs (shRNAs) for *Cyrano* KD. Since the shRNA sequences used in this study were not accessible, we were unable to further investigate this discrepancy. Of note, *Cyrano* was also found as a candidate in an RNAi screen for pluripotency-related lncRNAs in murine ESCs that also used shRNA technology (Lin et al., 2015). Nevertheless, constraints on different approaches for loss-off-function studies were recently described, in particular, the comparison of screenings using CRISPR/Cas9 KO and shRNA-mediated KD showed weak correlations (Morgens et al., 2016). Moreover, the comparison of two different RNAi technologies showed poor reproducibility (Bhinder and Djaballah, 2013). CRISPR technology has gained more popularity in the last years and outperformed RNAi approaches with less noise and off-target effects (Evers et al., 2016). Hence, the readouts after modulation of transcript expression have to be validated carefully. Accordingly, we tested different approaches and cell types (mouse iPSCs, human iPSCs, and ESCs), which all showed the same effects. Thus, it is unlikely that our results are based on off-target or approach-dependent effects. It should be noted that, although unlikely given the high conservation of *Cyrano*, the previously described effects of shRNA-mediated KD of *Cyrano* may be unique to murine ESCs. But it is also unlikely that both shRNAs used by Smith et al. would show the same off-target effects, which is supported by their data showing that overexpression of miR-7-5p exhibits the same phenotype as *Cyrano* KD. Thus, there exists a currently unknown factor to explain the discrepancy between both studies.

We further investigated the suggested downstream mechanism via regulation of miR-7-5p. In line with previous reports, we found an upregulation of miR-7-5p after *Cyrano* inhibition. However, there was no evidence that miR-7-5p affects pluripotency in our systems as demonstrated in experiments with miR-7-5p mimics.

Cyrano was first described to be important for zebrafish embryogenesis and brain morphogenesis (Ulitsky et al., 2011), which goes along with the proposed role in self-renewal and maintenance of pluripotency of murine ESCs (Smith et al., 2017). In contrast to the study in zebrafish, it was recently shown that a genetic KO of *Cyrano* in fish did not influence embryogenesis, viability, or fertility. The lack of reproducibility of the zebrafish experiments is based on off-target effects of the two different morpholinos that were used to inhibit *Cyrano* (Goudarzi et al., 2019). In addition, *Cyrano* KO mice do not show defects in embryogenesis, viability, or fertility (Kleaveland et al., 2018), which one would expect if *Cyrano* was essential for the maintenance of PSCs.

Finally, global transcriptomic analysis revealed that loss of *Cyrano* has only very moderate effects in PSCs that are not related to know pluripotency factors. Moreover, despite the absence of *Cyrano*, human iPSCs can be readily differentiated into the three germ layers which require the iPSCs to be truly pluripotent.

In summary, contradictory to previous data, we did not detect any changes in the pluripotency of murine and human iPSCs and human ESCs after *Cyrano* inhibition. Our different approaches to silence *Cyrano* in PSCs are highly consistent, firmly demonstrating that *Cyrano* is not regulating pluripotency. Nonetheless, the high degree of conservation and the high expression in PSCs assume an important cellular function of *Cyrano* for whose study we generated state-of-the-art *in vitro* tools.

EXPERIMENTAL PROCEDURES

Detailed methods are provided in Supplemental Experimental Procedures.

Murine iPSC Culture and Generation

Murine iPSCs have been reprogrammed from OG2 mice expressing EGFP under the control of an Oct3/4 promoter (Kensah et al., 2013). The murine iPSCs were grown on irradiated mitotic inactive mouse embryonic fibroblasts.

To knock out the *Cyrano* gene in iPSCs, the dual gRNA CRISPR/Cas9 approach was used (Heckl et al., 2014). The first exon of *Cyrano* was excised with two gRNAs knocking out both murine transcripts.

Human iPSC Culture and Generation

CRISPRi iPSCs (Mandegar et al., 2016) were cultured on Matrigel Growth Factor Reduced (Corning) in mTesR (STEMCELL Technologies) and passaged when confluent with Accutase (STEMCELL Technologies) in mTeSR supplemented with 10 μM Y-27632 2HCI (Selleckchem).

The gRNA design, cloning, and nucleofection were performed as described previously (Mandegar et al., 2016). For KD, induction cells were treated with 2 μM doxycycline for at least 3 days.

Human ESC Culture

MIXL1-GFP human ESC (Davis et al., 2008) were cultured on Geltrex (Thermo Fisher Scientific) in homebrewed E8 medium and passaged with Accutase (Gibco), seeded in 10 μM Y-27632 (Tocris). Cells came from a conventional feeder-based culture, expanded on Geltrex for two passages before being used for experiments.

Gene Expression

Total RNA of cultured cells was isolated using peqGOLD TriFast (VWR Life Science, Radnor, PA, USA) according to the manufacturer's instructions. RNA was DNase treated using RNase-free DNase set (QIAGEN), and 100 to 1,000 ng were reverse transcribed using Biozym cDNA synthesis kit.

To analyze miRNA expression levels 100 ng RNA was reverse transcribed using a iScript select cDNA synthesis kit (Bio-Rad) and specific TaqMan probes (hsa-miR-7-5p ID 005723_mat and RNU48 ID 001006, Thermo Fisher Scientific).

Real-time quantitative PCR was performed in CFX384 Touch Real-Time PCR Detection System (Bio-Rad) or QuantStudio 7 Flex System (Applied Biosystems). For mRNA and lncRNA expression analysis, iQ SYBR Green Supermix (Bio-Rad) was used and Absolute Blue qPCR Mix (Thermo Fisher Scientific) was used for miRNA expression analysis.

Absolute Quantification

The copy number of *Cyrano* was quantified by qPCR and a plasmid standard curve as described previously (Feretzaki et al., 2019).

Growth Curve

iPSCs (1×10^5) were seeded on Matrigel, and the following day doxycycline treatment was started and cells were counted for 5 consecutive days with Countess II (Invitrogen).

Alkaline Phosphatase Staining

The iPSCs were stained with the Alkaline Phosphatase Detection Kit (Millipore) according to the manufacturer's guidelines. Images were acquired with an Eclipse Ti-U fluorescence microscope (Nikon) and NIS Elements BR 3.26 (Nikon) software.

Flow Cytometry

For flow cytometry, cells were harvested, stained, then washed. Measurement was performed at Guava easyCite 5 flow cytometer (Millipore) and data analyzed with FlowJo (BD).

Human ESCs were fixed and permeabilized with FIX&PERM kit 1000 (Nordic MUbio). Staining was performed as described above.

Immunocytochemistry

iPSCs were washed, permeabilized, and incubated with primary and secondary antibodies.

RNA FISH

RNA FISH was performed using a ViewRNA Cell plus Assay (Thermo Fisher Scientific) according to the manufacturer's guidelines in Nunc Lab-Tek eight-well chamber slides (Merck) with a specific *Cyrano* probe (ID VA1-3020478-VCP, Thermo Fisher Scientific). Images were acquired using a Leica SP8 confocal microscope and LAS X (Leica) software.

Trilineage Differentiation

Differentiation was performed using a STEMdiff Trilineage Differentiation Kit (STEMCELL Technologies) according to manufacturer's guidelines.

Transfection of siRNA

Downregulation was achieved by transfecting 200 nM siRNAs (Eurofins) with Lipofectamine 2000 (Invitrogen) according to the manufacturer's guidelines.

PCR

PCR was performed using a HotStar Mastermix Kit (QIAGEN) according to the manufacturer's guidelines in 10 μL reaction. PCR products were resolved by agarose gel electrophoresis (0.8%–1.2% agarose gel in 1× TAE).

Sanger Sequencing

To verify sequences, DNA bands were cut from an agarose gel and DNA was extracted via the QIAquick Gel Extraction Kit (QIAGEN). Five to 10 ng/μL PCR product or 50–100 ng/μL plasmid DNA were brought to 15 μL volume premixed with 2 μL primer (10 μM) and sent to Eurofins for sequencing.

RNA-Seq

RNA was isolated using a miRNeasy mini kit (QIAGEN) according to the manufacturer's guidelines. Sample preparation and data processing are described in Supplemental Information.

Statistics

Statistical analyses were performed using an unpaired Student's t test. The results shown were obtained by at least three measurements (mean ± standard deviation [SD]). Statistical analysis was carried out using GraphPad Prism 8.

Data and Code Availability

RNA-seq data (GEO: GSE150421) are available in the Gene Expression Omnibus.

SUPPLEMENTAL INFORMATION

Supplemental Information can be found online at https://doi.org/10.1016/j.stemcr.2020.05.011.

AUTHOR CONTRIBUTIONS

CONFLICTS OF INTERESTS

ACKNOWLEDGMENTS

REFERENCES

Agarwal, V., Bell, G.W., Nam, J.W., and Bartel, D.P. (2015). Predicting effective microRNA target sites in mammalian mRNAs. eLife *4*, 1–38.

Bär, C., Chatterjee, S., and Thum, T. (2016). Long noncoding RNAs in cardiovascular pathology, diagnosis, and therapy. Circulation *134*, 1484–1499.

Beby, F., and Lamonerie, T. (2013). The homeobox gene Otx2 in development and disease. Exp. Eye Res. *111*, 9–16.

Beermann, J., Piccoli, M.T., Viereck, J., and Thum, T. (2016). Noncoding RNAs in development and disease: background, mechanisms, and therapeutic approaches. Physiol. Rev. *96*, 1297–1325.

Bhinder, B., and Djaballah, H. (2013). Systematic analysis of RNAi reports identifies dismal commonality at gene-level and reveals an unprecedented enrichment in pooled shRNA screens. Comb. Chem. High Trooughput Screen. *16*, 665–681.

Bilic, J., and Belmonte, J.C.I. (2012). Concise review: induced pluripotent stem cells versus embryonic stem cells: close enough or yet too far apart? Stem Cells *30*, 33–41.

Davis, R.P., Ng, E.S., Costa, M., Mossman, A.K., Sourris, K., Elefanty, A.G., and Stanley, E.G. (2008). Targeting a GFP reporter gene to the MIXL1 locus of human embryonic stem cells identifies human primitive streak-like cells and enables isolation of primitive hematopoietic precursors. Blood *111*, 1876–1884.

Evers, B., Jastrzebski, K., Heijmans, J.P.M., Grernrum, W., Beijersbergen, R.L., and Bernards, R. (2016). CRISPR knockout screening outperforms shRNA and CRISPRi in identifying essential genes. Nat. Biotechnol. *34*, 631–633.

Feretzaki, M., Nunes, P.R., and Lingner, J. (2019). Expression and differential regulation of human TERRA at several chromosome ends. RNA *25*, 1470–1480.

Goudarzi, M., Berg, K., Pieper, L.M., and Schier, A.F. (2019). Individual long non-coding RNAs have no overt functions in zebrafish embryogenesis, viability and fertility. eLife *8*, 1–17.

Heckl, D., Kowalczyk, M.S., Yudovich, D., Belizaire, R., Puram, R.V., McConkey, M.E., Thielke, A., Aster, J.C., Regev, A., and Ebert, B.L. (2014). Generation of mouse models of myeloid malignancy with combinatorial genetic lesions using CRISPR-Cas9 genome editing. Nat. Biotechnol. *32*, 941–946.

Kensah, G., Roa Lara, A., Dahlmann, J., Zweigerdt, R., Schwanke, K., Hegermann, J., Skvorc, D., Gawol, A., Azizian, A., Wagner, S., et al. (2013). Murine and human pluripotent stem cell-derived cardiac bodies form contractile myocardial tissue in vitro. Eur. Heart J. *34*, 1134–1146.

Kim, J., Abdelmohsen, K., Yang, X., De, S., Grammatikakis, I., Noh, J.H., and Gorospe, M. (2016). LncRNA OIP5-AS1/cyrano sponges RNA-binding protein HuR. Nucleic Acids Res. *44*, 2378–2392.

Kleaveland, B., Shi, C.Y., Stefano, J., and Bartel, D.P. (2018). A network of noncoding regulatory RNAs acts in the mammalian brain. Cell *174*, 350–362.e17.

Li, M., and Belmonte, J.C.I. (2017). Ground rules of the pluripotency gene regulatory network. Nat. Rev. Genet. *18*, 180–191.

Lin, N., Chang, K., Li, Z., Gates, K., Rana, Z.A., Zhang, D., Han, T., Yang, C., Cunningham, T.J., Head, R., et al. (2015). An evolutionarily conserved long noncoding RNA TUNA controls pluripotency and neural lineage commitment. Mol. Cell *53*, 1005–1019.

Mandegar, M.A., Huebsch, N., Frolov, E.B., Shin, E., Truong, A., Olvera, M.P., Chan, A.H., Miyaoka, Y., Holmes, K., Spencer, C.I., et al. (2016). CRISPR interference efficiently induces specific and reversible gene silencing in human iPSCs. Cell Stem Cell *18*, 541–553.

Morgens, D.W., Deans, R.M., Li, A., and Bassik, M.C. (2016). Systematic comparison of CRISPR/Cas9 and RNAi screens for essential genes. Nat. Biotechnol. *34*, 634–636.

Nelson, B.R., Makarewich, C.A., Anderson, D.M., Winders, B.R., Troupers, C.D., Wu, F., Reese, A.L., McAnally, J.R., Chen, X., Kavalali, E.T., et al. (2016). A peptide encoded by a transcript annotated as long noncoding RNA enhances SERCA activity in muscle. Science *351*, 271–275.

Smith, K.N., Starmer, J., Miller, S.C., Sethupathy, P., and Magnuson, T. (2017). Long noncoding RNA moderates microRNA activity to maintain self-renewal in embryonic stem cells. Stem Cell Reports *9*, 108–121.

Takahashi, K., and Yamanaka, S. (2006). Induction of pluripotent stem cells from mouse embryonic and adult fibroblast cultures by defined factors. Cell *126*, 663–676.

Ulitsky, I., Shkumatava, A., Jan, C.H., Sive, H., and Bartel, D.P. (2011). Conserved function of lincRNAs in vertebrate embryonic development despite rapid sequence evolution. Cell *147*, 1537–1550.

Wang, M., Liu, Y., Li, C., Zhang, Y., Zhou, X., and Lu, C. (2019). Long noncoding RNA OIP5-AS1 accelerates the ox-LDL mediated vascular endothelial cells apoptosis through targeting GSK-3β via recruiting EZH2. Am. J. Transl. Res. *11*, 1827–1834.